

On the use of slow manifolds in molecular and geophysical fluid dynamics

Tobias Hundertmark^{1,a} and Sebastian Reich¹

Institut für Mathematik, Am Neuen Palais 10, 14469 Potsdam, Germany

Abstract. Constraints typically arise from the elimination of high frequency oscillations in mechanical systems. Examples are provided by bond constraints in molecular simulations and incompressibility constraints in fluid dynamics. A key issue is the accuracy of constrained dynamics with regard to the full dynamics. In this review we focus on the smooth solution components and discuss the concept of slow manifold and soft constraints in molecular and geophysical fluid dynamics. While the formal mathematical derivation of constraints is the same for both molecular and fluid dynamics, the predominant numerical techniques for dealing with constraints are different in the two fields. Semi-implicit time-stepping methods are often used in geophysical fluid dynamics while explicitly enforced constraints are more common in molecular dynamics.

1 Introduction

We consider mechanical systems with stiff potential contributions, which give rise to rapid oscillations compared to the slow time-scales of interest. To keep the exposition as transparent as possible, we will mostly consider N degrees of freedom systems with a single fast degree of freedom of type

$$\frac{dq}{dt} = M^{-1}p, \quad (1)$$

$$\frac{dp}{dt} = -\nabla_q V(q) - \varepsilon^{-2}G(q)^T g(q), \quad (2)$$

where $q \in \mathbb{R}^N$ is the vector of particle positions, $p \in \mathbb{R}^N$ is the vector of particle momenta, $M \in \mathbb{R}^{N \times N}$ is a positive-definite mass matrix, $V : \mathbb{R}^N \rightarrow \mathbb{R}$ is a smooth potential, $g(q) : \mathbb{R}^N \rightarrow \mathbb{R}$ is an appropriate convex functions, $G(q) = g_q(q) \in \mathbb{R}^{1 \times N}$ denotes the Jacobian of g , and $0 < \varepsilon \ll 1$ is a small constant. The system (1)-(2) conserves the energy (Hamiltonian)

$$\mathcal{H}(q, p) = \frac{1}{2}p^T M^{-1}p + V(q) + \frac{1}{2\varepsilon^2}g(q)^2.$$

^a e-mail: sreich@math.uni-potsdam.de

If the system (1)-(2) is solved by the explicit Störmer-Verlet method [1,2]

$$p^{n+1/2} = p^n - \frac{\Delta t}{2} [\nabla_q V(q^n) + \varepsilon^{-2} G(q^n)^T g(q^n)], \quad (3)$$

$$q^{n+1} = q^n + \Delta t M^{-1} p^{n+1/2}, \quad (4)$$

$$p^{n+1} = p^{n+1/2} - \frac{\Delta t}{2} [\nabla_q V(q^{n+1}) + \varepsilon^{-2} G(q^{n+1})^T g(q^{n+1})] \quad (5)$$

with step-size $\Delta t > 0$, linear stability requires that

$$\Delta t = \mathcal{O}(\varepsilon),$$

which can impose a severe step-size restriction when one is primarily interested in the slow dynamics on time-scales of order $\mathcal{O}(\varepsilon^0)$ or longer. In the limit $\varepsilon \rightarrow 0$, the slow dynamics can be recovered from the constrained system [1,2]

$$\frac{dq}{dt} = M^{-1} p, \quad (6)$$

$$\frac{dp}{dt} = -\nabla_q V(q) - G(q)^T \lambda, \quad (7)$$

$$0 = g(q), \quad (8)$$

where the Lagrange multiplier $\lambda \in \mathbb{R}$ is determined from

$$\begin{aligned} \frac{d^2}{dt^2} g(q) &= \frac{d}{dt} G(q) M^{-1} p \\ &= G(q) M^{-1} [-\nabla_q V(q) - G(q)^T \lambda] + p^T M^{-1} g_{qq}(q) M^{-1} p. \end{aligned}$$

Here $g_{qq}(q) \in \mathbb{R}^{N \times N}$ denotes the Hessian of g . For this limit to hold (see, e.g. [5,3]), we need to require that the initial conditions $(q_\varepsilon(0), p_\varepsilon(0))$ are chosen such that

$$\mathcal{H}(q_\varepsilon(0), p_\varepsilon(0)) = \mathcal{O}(\varepsilon^0)$$

as well as

$$g(q_\varepsilon(0)) = \mathcal{O}(\varepsilon^2), \quad G(q)p = \mathcal{O}(\varepsilon)$$

meaning that the energy in the fast degree of freedom vanishes as $\varepsilon \rightarrow 0$. The later assumption is not realistic for molecular simulations and correcting force terms arise in general [5,3,4], which we do not discuss further in this paper. The interested reader is referred to the contribution of [6] in this volume for a discussion of constraints in the context of equilibrium statistical mechanics. Equations (6)-(8) can be solved by the SHAKE/RATTLE method and the step-size can now be chosen independent of ε .

In fluid dynamics a similar situation occurs. In a first instance, barotropic ideal fluid dynamics can be formulated as a continuum mechanical system where the forces depend only on the density of the fluid [7]. This special force structure allows one to reduce the equations of motion (similar to the reduction possible for rigid body motion) to the compressible Euler fluid equations

$$v_t = -v \cdot \nabla_x v - \nabla_x \pi(\rho), \quad (9)$$

$$\rho_t = -\nabla_x \cdot (\rho v), \quad (10)$$

where $\rho(x, t)$ denotes the density of the fluid, $\pi(\rho)$ its pressure as a function of density, and $v(x, t)$ its velocity field. Here $x \in \mathbb{R}^d$, $d = 2, 3$ represents the (now) independent

spatial coordinates in two or three dimensions. The limit of incompressibility gives rise to a holonomic constraint similar to $g(q)$ in terms of the Lagrangian formulation of ideal fluid dynamics which, in terms of (9)-(10), becomes

$$v_t = -v \cdot \nabla_x v - \nabla_x \pi, \quad (11)$$

$$0 = \nabla_x \cdot v, \quad (12)$$

under the assumption of a homogeneous initial fluid density. Pressure takes now the role of a Lagrange multiplier determined from

$$0 = \nabla_x \cdot v_t = \nabla_x \cdot [-v \cdot \nabla_x v - \nabla_x \pi]. \quad (13)$$

It should be noted that (12) corresponds to the velocity constraint $G(q)p = 0$ and that (13) itself is a consequence of the holonomic constraint that the fluid density is kept constant in space and time.

Geophysical fluid dynamics requires the augmentation of these equations by additional forcing terms and an equation for temperature [7,8]. However, these more complex equations are not necessary for the purpose of this paper.

In many instances, enforcing constraints of type (8) or (12), respectively, is too restrictive since the parameter value ε for the physical system under consideration is not so small as to allow the formal mathematical limit $\varepsilon \rightarrow 0$ to be taken. Two strategies to deal with such situations have been developed. The first is to replace the constraints by a more accurate representations of the manifold on which the slow dynamics takes place (see, e.g. [15,9]). The second approach is to use linearly implicit, also called semi-implicit, time-stepping methods for the unapproximated equations of motion (see, e.g. [11,8]).

2 Stiff spring pendulum

The stiff spring model is used in molecular as well as geophysical fluid dynamics as a toy model to demonstrate the coupling between slow motion and rapid oscillations (see, e.g. [5,12]). In this section, we therefore discuss the concepts of slow manifolds and regularized equations of motion for a planar stiff spring pendulum

$$\frac{dq_x}{dt} = \frac{p_x}{m}, \quad \frac{dq_y}{dt} = \frac{p_y}{m}, \quad \frac{dp_x}{dt} = -k \frac{q_x}{r} (r - l), \quad \frac{dp_y}{dt} = -mg - k \frac{q_y}{r} (r - l),$$

where the coordinates are $q = (q_x, q_y)$, the momenta are $p = (p_x, p_y)$, and $r = \sqrt{q_x^2 + q_y^2}$. Here $l > 0$ is the equilibrium length of the stiff spring, $k \gg 1$ is the force constant, $m > 0$ is the body's mass, and g is the gravitational constant.

To gain more insight we reformulate the equations of motion in polar coordinates (θ, r) , where r is the radius, i.e. the length between the body and the fixed suspension, and θ is the angle between position vector and y -axis. Further, we define the radial momentum $p_r = mdr/dt$ and the angular momentum $p_\theta = mr^2 d\theta/dt$. The Hamiltonian function of the elastic pendulum is now given by

$$\mathcal{H}(q, p) = \frac{1}{2m} \left(p_r^2 + \frac{p_\theta^2}{r^2} \right) + \frac{1}{2} k (r - l)^2 - mgr \cos \theta.$$

with the corresponding Hamiltonian equations of motion

$$\frac{d\theta}{dt} = \frac{p_\theta}{mr^2} \quad (14)$$

$$\frac{dp_\theta}{dt} = -mgr \sin \theta \quad (15)$$

$$\frac{dr}{dt} = p_r/m \quad (16)$$

$$\frac{dp_r}{dt} = \frac{p_\theta^2}{mr^3} - k(r-l) + mg \cos \theta. \quad (17)$$

The stiff spring gives rise to rapid oscillations with frequency

$$\omega_S = \sqrt{\frac{k}{m}}.$$

We now formally set $\varepsilon^2 = 1/k$ and, in the limit $\varepsilon \rightarrow 0$, the constraints $g(q) = 0$ and $G(q)M^{-1}p = 0$ are now provided in terms of the general formulation (1)-(2) by

$$r(t) = l, \quad p_r(t) = 0$$

and the reduced equations of motion are given by (14)-(15), which corresponds to (6)-(8) in cartesian coordinates. The frequency of small angle pendulum motion is

$$\omega_P = \sqrt{\frac{g}{l}}$$

and $\omega_P \ll \omega_S$ for $0 < \varepsilon \ll 1$.

A more accurate representation of the slow motion on time-scales of order $\mathcal{O}(\varepsilon^0)$ is provided by the bounded derivative principle (see, e.g. [13,12])

$$\frac{dr}{dt} = \mathcal{O}(\varepsilon^2), \quad \frac{dp_r}{dt} = \mathcal{O}(\varepsilon^1).$$

Initial conditions which satisfy these conditions are said to be in nonlinear balance. Obviously, nonlinearly balanced initial conditions require here that $p_r(0) = 0$ and

$$r_{\text{NL}}(0) = l + k \left(\cos \theta(0) + \frac{p_\theta^2(0)}{ml^3} \right)$$

to leading order in $\varepsilon^2 = 1/k$. Once initialized in nonlinear balance, or close to it, the system will remain close to a nonlinearly balanced state [14] and, hence, the fast oscillations are controlled by the slow pendulum motion and a good approximation to the full dynamics could be made by the slow equations:

$$\frac{d\theta}{dt} = \frac{p_\theta}{mr^2}, \quad (18)$$

$$\frac{dp_\theta}{dt} = -mgr \sin \theta, \quad (19)$$

$$0 = p_r, \quad (20)$$

$$0 = \frac{p_\theta^2}{ml^3} - k(r-l) + mg \cos \theta. \quad (21)$$

The fast mode has thus been eliminated on the level of the continuous model. This could be seen as favorable for a numerical approach to the elastic pendulum, where

the time step of an explicit integration scheme is no longer restricted by the elastic motion. However, contrary to the hard constraints $p_r = 0$, $r = 0$, the modified constraint (21) is no longer holonomic since the angular momentum p_θ is involved. A standard holonomic constraints approach is possible once (21) is replaced by

$$0 = -k(r - l) + mg \cos \theta.$$

This approach corresponds to what is called soft or elastic constraints in [15,9]. See also the contribution of [10] in this volume.

In the following we discuss approaches of numerically solving the original, full equations without explicitly eliminating the fast mode. The advantage of implicit schemes, such as the implicit midpoint method, is that they are unconditionally stable with respect to linear fast and slow modes. On the other hand, they introduces fully implicit relations in linear and nonlinear terms which, in general, requires an iterative method for solving the resulting nonlinear equations. This is most unfavorable in situations where the calculation of the nonlinear terms is a computationally very expensive task, because iterative methods usually require multiple evaluations of these terms. Indeed, in practice, the implicit midpoint rule is neither widely used in the context of molecular dynamics nor for fluid dynamics simulations. Implicit methods can also suffer from nonlinear instabilities (see, e.g., [16]).

A plausible alternative is provided by linearly implicit (semi-implicit) one-step methods. A very simple scheme of that class can be constructed by using an explicit Euler step for the nonlinear term and an implicit midpoint discretization of the linearized stiff spring oscillations. The method can be written in the following algorithmic form:

$$\theta^{n+1} = \theta^n + \Delta t \frac{p_\theta^n}{m(r^n)^2} \quad (22)$$

$$p_\theta^{n+1} = p_\theta^n - \Delta t m g r^n \sin \theta^n \quad (23)$$

$$r^{n+1} = r^n + \Delta t \frac{p_r^{n+1/2}}{m} \quad (24)$$

$$p_r^{n+1} = p_r^n + \Delta t \left[\frac{(p_\theta^n)^2}{m(r^n)^3} + mg \cos \theta^n - k(r^{n+1/2} - l) \right], \quad (25)$$

where a midpoint value is defined by

$$X^{n+1/2} = \frac{X^n + X^{n+1}}{2}.$$

However, this method, while being linearly stable in the stiff spring oscillations for step-sizes $\Delta t = \mathcal{O}(\varepsilon^0)$, is still not suitable for molecular and geophysical fluids simulations since the time-reversibility of the equations of motion is lost.

We now demonstrate how to obtain a time-reversible linearly implicit time-stepping method using the concept of regularized equations [17]. We start by rewriting (24)-(25) as updates of the midpoint values

$$r^{n+1/2} = r^n + \frac{\Delta t}{2m} p_r^{n+1/2} \quad (26)$$

$$p_r^{n+1/2} = p_r^n + \frac{\Delta t}{2} (C^n - k(r^{n+1/2} - l)), \quad (27)$$

where we collected the explicit nonlinear terms in

$$C^n := \frac{(p_\theta^n)^2}{m(r^n)^3} + mg \cos \theta^n.$$

We substitute (27) into (26) and obtain a linearly implicit equation in $r^{n+1/2}$, i.e.

$$\left(1 + \frac{k\Delta t^2}{4m}\right) (r^{n+1/2} - l) = \hat{r}^{n+1/2} - l + \frac{\Delta t^2}{4} \frac{C^n}{m} \quad (28)$$

in which the explicit midpoint predictor is defined by a $\Delta t/2$ forward Euler step

$$\hat{r}^{n+1/2} = r^n + \frac{\Delta t}{2m} p_r^n.$$

The stability property of the implicit midpoint scheme guarantees that the eigenvalues of the numerical propagation matrix corresponding to the linear fast modes are on the unit circle independently of the size of the time step. The idea is to build this feature into a new variable, i.e. a *regularized radius* \tilde{r} . Hence we identify $\hat{r}^{n+1/2}$ with $r(t_{n+1/2})$ and $r^{n+1/2}$, as obtained from the implicit midpoint rule, with a regularized radius $\tilde{r}(t_{n+1/2})$, which is then determined by the equation

$$\left(1 + \frac{k\Delta t^2}{4m}\right) [\tilde{r} - r] = \frac{\Delta t^2}{4m} \left[\frac{p_\theta^2}{mr^3} - k(r - l) + mg \cos \theta \right]. \quad (29)$$

The equations of motion for the regularized spring pendulum are finally given by the system

$$\frac{d\theta}{dt} = \frac{p_\theta}{mr^2}, \quad (30)$$

$$\frac{dp_\theta}{dt} = -mgr \sin \theta, \quad (31)$$

$$\frac{dr}{dt} = \frac{p_r}{m}, \quad (32)$$

$$\frac{dp_r}{dt} = \frac{p_\theta^2}{mr^3} - k(\tilde{r} - l) + mg \cos \theta, \quad (33)$$

together with the additional (linear) equation (29) to be solved for the regularized radius \tilde{r} .

We can now apply a symmetric time-stepping method to the regularized equations which is explicit in the conservative forcing terms. A natural choice is the generalized Störmer-Verlet method [1,2], which applied to the regularized spring pendulum problem (30)-(33) and (29) yields:

First half step in momentum:

$$p_\theta^{n+1/2} = p_\theta^n - \frac{\Delta t}{2} mgr^n \sin \theta^n$$

$$p_r^{n+1/2} = p_r^n + \frac{\Delta t}{2} \left[\frac{(p_\theta^{n+1/2})^2}{m(r^n)^3} + mg \cos \theta^n - k(\tilde{r}^n - l) \right]$$

Full step in coordinates:

$$r^{n+1} = r^n + \Delta t \frac{p_r^{n+1/2}}{m}$$

$$\theta^{n+1} = \theta^n + \Delta t \frac{p_\theta^{n+1/2}}{m(r^{n+1/2})^2}$$

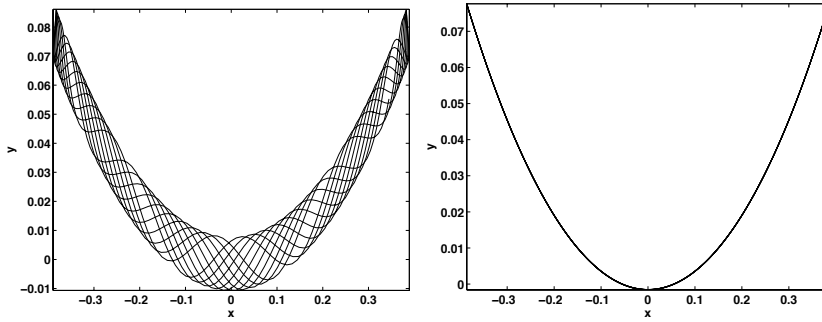


Fig. 1. Standard Störmer-Verlet simulations with $m = 1$, $l = 1$, $g = \pi^2$, $k = 10^2 \pi^2$, $\Delta t = 0.01$. Left panel: linear balance initial conditions $(\theta(0), p_\theta(0), r(0), p_r(0)) = (\pi/8, 0, 1, 0)$; Right panel: nonlinear balance initial conditions $(\theta(0), p_\theta(0), r(0), p_r(0)) = (\pi/8, 0, [1 + \varepsilon^2 \cos \theta_0], 0)$.

Second half step in momentum:

$$\begin{aligned}
 p_\theta^{n+1} &= p_\theta^{n+1/2} - \frac{\Delta t}{2} m g r^{n+1} \sin \theta^{n+1} \\
 \tilde{r}^{n+1} &= r^{n+1} + \left(1 + \frac{k \Delta t^2}{4m}\right)^{-1} \frac{\Delta t^2}{4m} \left[\frac{(p_\theta^{n+1})^2}{m(r^{n+1})^3} - k(r^{n+1} - l) + m g \cos \theta^{n+1} \right] \\
 p_r^{n+1} &= p_r^{n+1/2} + \frac{\Delta t}{2} \left[\frac{(p_\theta^{n+1/2})^2}{m(r^{n+1})^3} + m g \cos \theta^{n+1} - k(\tilde{r}^{n+1} - l) \right]
 \end{aligned}$$

For this example, the specific coupling of linear and nonlinear terms results in a completely explicit algorithm, but we must generally expect a *weakly* implicit scheme which converges quickly with only a few fixed point iterations, without the need of applying a more complicated Newton method.

Numerical methods are now implemented for a spring pendulum with mass $m = 1$, equilibrium spring length of $l = 1$ and gravitational constant $g = \pi^2$, as described in [12]. With this choice of parameters the frequency corresponding to the slow pendulum motion is $\omega_P = \pi$. The spring coefficient is chosen to be either $k = 10^2 \pi^2$ or $k = 100^2 \pi^2$. In the first case the stiff spring frequency is $\omega_S = 10 \pi$ which implies a ratio of $\varepsilon = 0.1$ and for the alternative choice we have a ten times larger $\omega_S = 100 \pi$ with ratio $\varepsilon = 0.01$. Numerical test use either the initial conditions (linear balance)

$$(\theta(0), p_\theta(0), r(0), p_r(0)) = (\pi/8, 0, 1, 0)$$

or the balanced initial conditions (nonlinear balance) given by

$$(\theta(0), p_\theta(0), r(0), p_r(0)) = (\pi/8, 0, 1 + \varepsilon^2 \cos \theta_0, 0).$$

A visual impression of the spring pendulum motion with $k = 10^2 \pi^2$ for both linearly and nonlinearly balanced initial conditions is given in Fig. 1. The results are computed by standard Störmer-Verlet method and step-size $\Delta t = 0.01$.

Fig. 2 demonstrates that the regularized Störmer-Verlet method produces stable results both in terms of energy as well as balanced dynamics for a time step $\Delta t = 0.01$, which violates the stability condition of Störmer-Verlet for the unregularized equations with stiff spring constant $k = 100^2 \pi^2$.

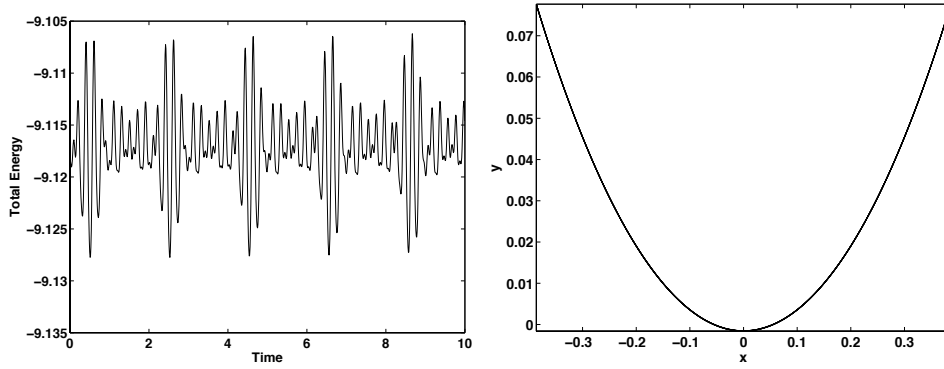


Fig. 2. Energy and positions of slow pendulum motion obtained from integrating the regularized Störmer-Verlet method for parameter values $\Delta t = 0.01$, $k = 100^2 \pi^2$.

3 General formulations

We now return to formulation (1)-(2) in Cartesian coordinates. The standard constrained manifold is provided by

$$\mathcal{M}_S = \{(q, p) \in \mathbb{R}^{2N} : g(q) = 0, G(q)M^{-1}p = 0\}$$

and the Lagrange multiplier in (6)-(8) is explicitly given by

$$\lambda(q, p) = (G(q)M^{-1}G(q)^T)^{-1} [G(q)M^{-1}p - \nabla_q V(q) + p^T M^{-1}g_{qq}(q)M^{-1}p]$$

A better approximation to the slow dynamics of (1) - (2) can be obtained by following [15,9], where the idea of self-consistent flexible constraints has been introduced. Instead of a hard or rigid constraints, it is required that the fast force contribution satisfies the balance condition

$$-\varepsilon^{-2}G(q)^T g(q) = -G(q)^T \lambda(q, p). \quad (34)$$

This condition can be understood as replacing the rigid constraint $g(q) = 0$ by the condition

$$g(q) = \varepsilon^2 \lambda(q, p) \quad (35)$$

and suggests to numerically integrate

$$M\dot{q} = p, \quad (36)$$

$$\dot{p} = -\nabla V(q) - G(q)^T \Lambda, \quad (37)$$

$$0 = g(q) - \varepsilon^{-2} \lambda(q, p) \quad (38)$$

instead of (6)-(8). The new Lagrange multipliers Λ are obtained by twice differentiating the constraint (38). Note that (38) is non-holonomic unless we set $p = 0$ in $\lambda(q, p)$. See [9] and also [18] for implementation details.

In order to derive a general regularized model based on the concept of self-consistent flexible constraints, we first write down a semi-implicit discretization of the system (1)-(2):

$$q^{n+1} = q^n + \Delta t M^{-1} p^{n+1/2}, \quad (39)$$

$$p^{n+1} = p^n - \Delta t \varepsilon^{-2} G(q^n)^T g^{n+1/2} - \Delta t \nabla_q V(q^n), \quad (40)$$

where $g^{n+1/2}$ is defined by

$$g^{n+1/2} = g\left(\frac{q^{n+1} + q^n}{2}\right).$$

We find that

$$g^{n+1/2} = g\left(\hat{q}^{n+1/2} - \frac{\Delta t^2}{4}M^{-1}\left(\varepsilon^{-2}G(q^n)^T g^{n+1/2} + \nabla_q V(q^n)\right)\right) \quad (41)$$

with predictor

$$\hat{q}^{n+1/2} = q^n + \frac{\Delta t}{2}p^n.$$

Formal Taylor series expansion yields

$$g^{n+1/2} \approx g\left(\hat{q}^{n+1/2}\right) - \frac{\Delta t^2}{4}G(q^n)M^{-1}\left(\varepsilon^{-2}G(q^n)^T g^{n+1/2} + \nabla_q V(q^n)\right) \quad (42)$$

and the linearly implicit problem

$$\left(1 + \frac{\Delta t^2}{4\varepsilon^2}G(q^n)M^{-1}G(q^n)^T\right)g^{n+1/2} = \hat{g}^{n+1/2} - \frac{\Delta t^2}{4}G(q^n)M^{-1}\nabla_q V(q^n) \quad (43)$$

with $\hat{g}^{n+1/2} = g(\hat{q}^{n+1/2})$.

Next we replace the fast term $g(q)$ by a regularized term $\tilde{g}(q)$ in the Hamiltonian system (1)-(2) to obtain

$$\frac{dq}{dt} = M^{-1}p, \quad (44)$$

$$\frac{dp}{dt} = -\varepsilon^{-2}G(q)^T \tilde{g}(q) - \nabla_q V(q), \quad (45)$$

where we require $\tilde{g}(q)$ to be the solution of a smoothing problem of the following form:

$$\mathcal{S}[\tilde{g} - g(q)] = -\frac{\alpha^2}{\varepsilon^2}\mathcal{R}. \quad (46)$$

Here the operator \mathcal{S} and $\alpha^2 \mathcal{R}$ are chosen in a way such that (46) mimics the linearly implicit problem (43) under the identification $g^{n+1/2} \rightarrow \tilde{g}$ and $\hat{g}^{n+1/2} \rightarrow g(q)$. We get

$$\mathcal{S} = 1 + \frac{\alpha^2}{\varepsilon^2}G(q)M^{-1}G(q)^T,$$

as well as

$$\mathcal{R} = G(q)M^{-1}\left[G(q)^T g(q) + \varepsilon^2 \nabla_q V(q)\right],$$

and

$$\alpha^2 = \Delta t^2/4,$$

respectively, for the parameter α .

Note, that $\tilde{g} = g(q)$ whenever the system's fast and slow force components are balanced which is expressed by

$$G(q)^T g(q) + \varepsilon^2 \nabla_q V(q) = 0,$$

which is equivalent to (35) with $p = 0$. Then all forces balance in the direction of the fast oscillations and the system remains close to that state.

A Störmer-Verlet discretization of the regularized system (44)-(45) yields a stable (provided $\alpha \geq \Delta t/2$), linearly implicit, and time-reversible algorithm:

Half step in momentum:

$$p^{n+1/2} = p^n - \frac{\Delta t}{2\varepsilon^2} G(q^n)^T \tilde{g}^n - \frac{\Delta t}{2} \nabla_q V(q^n)$$

Full step in coordinates:

$$q^{n+1} = q^n + \Delta t M^{-1} p^{n+1/2}$$

Regularization: ($G = G(q^{n+1})$)

$$\left(\frac{\varepsilon^2}{\alpha^2} + GM^{-1}G^T \right) \tilde{g}^{n+1} = \frac{\varepsilon^2}{\alpha^2} g(q^{n+1}) - \varepsilon^2 GM^{-1} \nabla V(q^{n+1})$$

Second half step in momentum:

$$p^{n+1} = p^{n+1/2} - \frac{\Delta t}{2\varepsilon^2} G(q^{n+1})^T \tilde{g}^{n+1} - \frac{\Delta t}{2} \nabla_q V(q^{n+1}).$$

It is straightforward to extend these ideas to vector-valued $g(q)$.

Following [17], the regularized formulation for the Euler equations (9)-(10) is provided by

$$\begin{aligned} v_t &= -v \cdot \nabla_x v - \nabla_x \tilde{\pi}, \\ \rho_t &= -\nabla_x \cdot (\rho v), \end{aligned}$$

with regularized pressure determined by the elliptic partial differential equation

$$[1 - \alpha^2 \nabla_x \cdot \rho \nabla_x] [\tilde{\pi} - \pi(\rho)] = \alpha^2 \nabla_x \cdot (\rho [v \cdot \nabla_x v + \nabla_x \pi(\rho)]).$$

These formulations are well-suited for Störmer-Verlet type time-stepping methods using semi-Lagrangian techniques for the (force free) transport part. See [19,20]. The implementation of soft constraints for the Euler equations (9)-(10) would amount to replacing (12) by

$$0 = \frac{\partial}{\partial t} \{ \nabla_x \cdot (\rho [v \cdot \nabla_x v + \nabla_x \pi(\rho)]) \}. \quad (47)$$

It would be of interest to discuss popular constraint formulations such as the anelastic and pseudo-incompressible approximation [8] in the light of (47).

4 Conclusions

Linearly implicit methods are widely used in computational fluid dynamics. Explicitly filtered equations (which amounts to enforcing some sort of constraints on the fluid equations) are also widely used but are not always suitable in particular for operational weather forecasting. On the other hand, constraints are often used in molecular dynamics for removing bond vibrations while implicit (or linearly implicit) methods can hardly be found. We have summarized work that demonstrates that both approaches are, in fact, closely related and that both communities could benefit from an exchange of algorithmic ideas.

While constraints explicitly remove fast vibrations from the system at the price of having to solve nonlinear equations, regularized equations artificially slow fast

oscillations down such that explicit time-stepping methods can be applied. The implementation of regularized equations then leads to linearly implicit time-stepping methods which are time-reversible but not symplectic. This can potentially lead to a drift in total energy in long time molecular dynamics simulations. Artificial resonances between the slowed-down fast vibrations and other natural frequencies of the system might also occur for conservative systems with no clear scale separation.

References

1. E. Hairer, Ch. Lubich and G. Wanner, *Geometric Numerical Integrators* (Springer-Verlag, Berlin 2006)
2. B. Leimkuhler and S. Reich, *Simulating Hamiltonian Dynamics* (Cambridge University Press, Cambridge 2004)
3. F. Bornemann, *Homogenization in Time of Singularly Perturbed Systems*, (Springer-Verlag, Berlin 1998)
4. S. Reich, *Physica D* **138**, (2000) 210–224
5. G. Benettin, L. Galgani and A. Giorgilli, *Communications in Mathematical Physics* **113**, (1987) 87–103
6. P. Echenique, C.N. Cavaotto and P. García-Risueño, *Eur. Phys. J. ST*, this issue
7. R. Salmon, *Lectures on Geophysical Fluid Dynamics* (Oxford University Press, Oxford 1998)
8. D.R. Durran, *Numerical Methods for Fluid Dynamic: With Applications to Geophysics*, (Springer-Verlag, New York 2010)
9. J. Zhou, S. Reich and B.R. Brooks, *J. Chem. Phys.* **112**, (2000) 7919–7929
10. R.D. Skeel and S. Reich, *Eur. Phys. J. ST*, this issue
11. A. Robert, *Jpn. Meteor. Soc.* **60**, (1982) 319–325
12. P. Lynch, *Large-Scale Atmospheric-Ocean Dynamics: Vol II: Geometric Methods and Models*, (Cambridge University Press, Cambridge 2002) 64–108
13. N. Kopell, *Physica D* **14**, (1985) 203–215
14. D. Wirosoetisno, *Adv. Diff. Eq.* **9**, (2004) 177–196
15. S. Reich, *Physica D* **89**, (1995) 28–42
16. T. Schlick, *Molecular Modelling and Simulation: An Interdisciplinary Guide*, (Springer-Verlag, New York 2010)
17. N. Wood, A. Staniforth and S. Reich, *Atmospheric Science Letters* **7**, (2006) 21–25
18. B. Hess, H. Saint-Martin and H.J.C. Berendsen, *J. Chem. Phys.* **116**, (2002) 9602–9610
19. T. Hundertmark and S. Reich, *Quarterly J. Royal. Meteorol. Soc.* **133** (2007) 1575–1587
20. A. Staniforth, N. Wood and S. Reich, *Quarterly J. Royal. Meteorol. Soc.* **132** (2006) 3107–3116